

RADIATION PROTECTION STUDIES FOR THE FRONT-END OF THE 3.5 GEV SPL AT CERN

Matteo Magistris, Egidio Mauro* and Marco Silari

* Corresponding author: Tel.+41227675280; E-mail address: egidio.mauro@cern.ch

CERN, CH-1211 Geneve 23, Switzerland

CERN is presently designing a Superconducting Proton Linac (SPL) accelerating H^- ions to energy of 3.5 GeV and beam power of up to 4 MW. The ultimate goal of this accelerator is the production of intense neutrino beams. The SPL is also intended to replace the present CERN injectors, the 50 MeV linac and the 1.4 GeV booster used for injecting into the 26 GeV proton synchrotron (PS). A conceptual design has also recently been started to replace the PS with a new 50 GeV synchrotron. The design of the first 160 MeV section of the SPL is well along as is the shielding study, which has been focused on three possible scenarios: the installation in an existing hall, in the building housing the present linac and in a future purpose-built tunnel (which will be referred to as "green field" solution). A shielding design was first carried out via analytical calculations. Next, extensive Monte Carlo simulations with the latest version of the FLUKA code were performed to investigate the propagation of neutrons in the existing buildings and to evaluate the environmental impact.

1. Introduction

A 160 MeV H^- linear accelerator, called Linac4 [1], is being designed at CERN to replace the present 50 MeV linac (Linac2) as injector to the Proton Synchrotron Booster (PSB). Linac4 will provide the conditions to double the intensity of the beam from the PSB. Moreover, this new linac constitutes an essential component of any of the envisaged LHC upgrade scenarios and could open the way to future extensions of the CERN accelerator complex. In one of these upgrade scenarios, Linac4 would be used as the front-end of the future multi-GeV, multi MW superconducting Proton Linac (SPL) [2,3]. The SPL is intended to produce intense neutrino beams and to replace the 1.4 GeV PSB injecting into the 26 GeV Proton Synchrotron (PS). A conceptual design was also recently started to replace the PS with a new 50 GeV synchrotron (called PS2). In this case the SPL will inject protons into PS2. The layout of these new

LHC injectors is shown in Fig. 1

The design of Linac4 is well advanced and its main parameters are based on the requirements for PSB injection. It will operate at 2 Hz, with a peak current of 40 mA and a pulse length of 0.4 ms. These parameters correspond to approximately 0.1% duty cycle and 0.032 mA average current or 2×10^{14} protons per second, which is equivalent to 5.1 kW beam power at the top energy of 160 MeV.

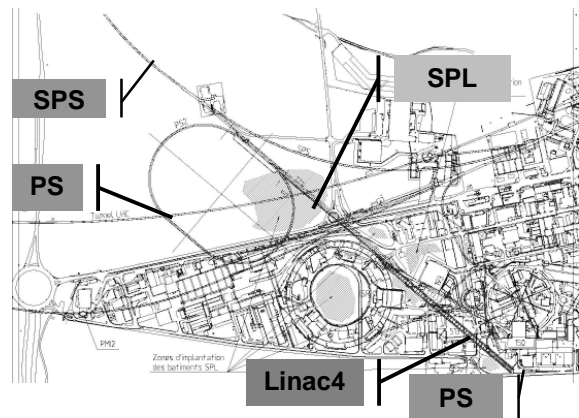


Fig 1: New LHC injector project.

The overall architecture of Linac4 is schematically shown in Fig. 2. The ion source is followed by a Radio Frequency Quadrupole (RFQ), a chopper line and the main linear accelerator structure. Three types of accelerating structures bring the energy to 160 MeV: a Drift Tube Linac (DTL) up to 40 MeV, a Cell-Coupled Drift Tube Linac (CCDTL) up to 90 MeV and finally a Side Coupled Linac (SCL) to the final energy. A long transfer line equipped with debunching and collimation sections connects Linac4 to the existing Linac2 transfer line. Three possible scenarios for the installation of the Linac4 were studied:

- 1) the installation in an existing hall;
- 2) the installation in the building housing the present linac with little additional shielding to the existing structure;
- 3) a green field solution.

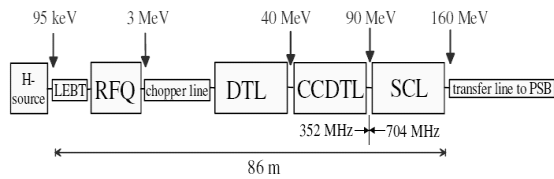


Fig 2: Schematic view of Linac4.

The shielding design for Linac4 in an existing hall has been studied in a previous paper[4]. This paper describes the Monte Carlo simulations performed to assess the effectiveness of the additional shielding needed in the second scenario, to optimize the waveguides ducts and to estimate the possible inhalation dose received by the workers from air activation in the green field solution.

2. Installation of Linac4 in an existing building with additional shielding

In modern linear accelerators, the design maximum beam loss is below 1 W/m. Losses below this threshold generate very low values of induced radioactivity such that hands-on maintenance on the accelerator is still possible. The beam dynamics and the apertures in Linac4 have been optimised to keep losses below 1 W/m at the SPL having a beam duty cycle of 5 %. The same loss level was also taken as guideline for the shielding calculations of Linac4 as the injector for PSB. This assumption leads to a safety factor of about 50, which is the ratio of the SPL and PSB duty cycles. Therefore, the proposed shielding design is appropriate for Linac4 to be used as the injector to PSB and it is rather conservative as used for the front-end of SPL.

In reality beam losses will not be equally distributed along the accelerator, but will typically occur in the aperture restrictions of quadrupoles. Other critical spots are the bending sections of the transfer line, where particles outside the energy acceptance of the bending will be lost on the vacuum chamber. In order to have a realistic loss configuration, in the following it is assumed that constant losses of 10 W every 10 m occur at selected points along the accelerator. In terms of shielding requirements this loss distribution is approximately equivalent to a uniform loss of 1 W/m.

As shown in Fig. 3, one of the most critical issues with the installation of Linac4 in the existing building is its proximity to the ion injector Linac3. At present Linac3 is shielded from the Linac2 radiation by "molasse" with a density of 2.4 g/cm³ which has the following composition: O (49,5%), Si (19,8%), Al (6,4%), K (1,8%), Fe (3,9%), Mg (3,2%), Na (0,5%),

Ca (9,3%), Mn (0,1%) and C (5%). This is used at 3 to 6 m thickness, depending on location. The section of Linac4 which is closest to Linac3 is where the energy increases from 140 to 160 MeV.

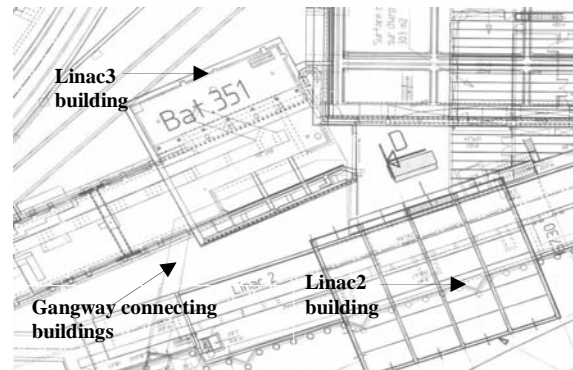


Fig 3: Schematic overview of the Linac2 and Linac3 buildings.

The high energy section and the transfer line of Linac4 were precisely modelled with the radiation transport code FLUKA [5,6]. The earth shielding separating the accelerator from Linac3 was implemented in FLUKA with the actual thickness. A 40 cm thick layer of concrete was added to the adjacent Linac2 wall to enhance the shielding.

Fig. 4 shows the geometry implemented in the simulation: the high energy section, the transfer line and the technical gallery of Linac4, the Linac3 external wall and the earth between the two accelerators.

The layout of the simulation includes the following structures (heights are given with reference to the tunnel floor):

- The part of the building housing the high energy (140-160 MeV) section of the accelerator, consisting of
 - the 14 m long, 3.5 m wide and 3.5 m high accelerator tunnel, with the 100 cm thick concrete shield on the left side, an additional 40 cm thick concrete shield on the right side (i.e., towards Linac3), the 100 cm thick concrete roof (the accelerator beam axis is at 126 cm height)
 - the 14 m long technical gallery on the left side of the accelerator at 170 cm height
 - the 30 cm thick concrete wall on the left side of the technical gallery
 - the 30 cm thick concrete floor of the accelerator tunnel
 - the building roof made of iron (1 cm thickness, 10.6 m height)
- The measurement tunnel, which corresponds to the first part of the transfer line, consisting of

- the 8.6 m long, 3.5 m wide and 6.1 m high measurement tunnel, with the 100 cm thick concrete shield on the left side, an additional 40 cm thick concrete shield on the right side and the 100 cm thick concrete roof
- the 30 cm thick concrete floor
- the 8.6 m long, 1.5 m wide and 5.5 m high tunnel on the left side of the measurement tunnel with the 20 cm thick concrete roof and the 20 cm thick concrete wall
- the earth above these tunnels, up to 650 cm height in the first metre and 750 cm height in the remaining 7.6 metres (consequently the first metre of the measurement tunnel is not underground).
- The second part of the transfer tunnel (i.e., downstream of the measurement tunnel), consisting of
 - the 3.3 m long, 3.5 m wide and 2.5 m high initial section, with the 100 cm thick concrete shield on the left side, an additional 40 cm thick concrete shield on the right side, the 100 cm thick concrete roof
 - the 30 cm thick concrete floor
 - the 5.5 m high and 6.3 m wide part of this building housing the tunnel with a 20 cm thick concrete roof and a 20 cm thick concrete left wall
 - the earth up to 750 cm height.
- The building housing the linac3 accelerator and the earth between the two accelerators, consisting of
 - the wall of the building 50 cm thick, made of concrete and tilted with respect to the shield on the right side of the Linac2 accelerator tunnel
 - the first part of the Linac3 building (closest to the first 10 metres of the Linac2 tunnel), which is 750 cm high and it is not underground, while the second part (closest to the final part of the accelerator and the transfer line) is 570 cm high and it is underground
 - the earth between the two buildings, defined as a tilted plane with respect to the floor of the accelerator. The plane reaches a maximum height of 610 cm in the first 14 metres, it is 650 cm high between 14 and 15 metres and 750 cm high in the remaining part.

The same FLUKA geometry was used for two separate sets of simulations, namely to predict the prompt radiation in Linac3 near the high energy section (140 MeV) and near the transfer line (160 MeV) of Linac4.

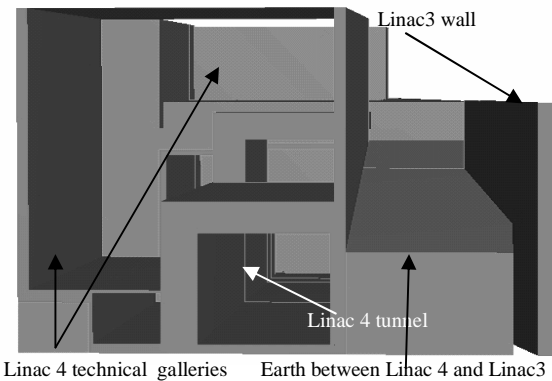


Fig 4: FLUKA geometry plotted with SimpleGeo [7]: cross sectional view of the Linac4 building and the wall of Linac3 building. The view is looking downstream of the tunnel, towards the high-energy end of the linac.

Beam losses were simulated as a 10 W proton beam hitting a $5 \times 5 \times 5 \text{ cm}^3$ copper target, which represents a magnet coil or yoke. Copper was chosen as representative of other materials with similar density (e.g., iron and stainless steel).

The first set of simulations was dedicated to study the stray radiation in the part of the Linac3 building close to the 140 MeV section of the Linac4. The ambient dose equivalent rate $H^*(10)$ was scored both on the ground floor of the Linac3 building - in the technical gallery - and at an height between 490 cm and 570 cm - on the upper floor. The dose rate is expected to be less than $1 \mu\text{Sv/h}$ in the technical gallery and up to $100 \mu\text{Sv/h}$ on the upper floor of the Linac3 building (Fig. 5). The reason for such a high dose rate can be ascribed to the insufficient amount of earth shielding between these two buildings (Fig. 4)

In the second set of simulations, the stray radiation in the part of the Linac3 building close to the transfer line of Linac4 was studied. The ambient dose equivalent rate $H^*(10)$ was scored in the Linac3 building on the ground floor, on the first floor and at an height between 730 cm and 810 cm. The latter location corresponds to the roof of the building, where the gangway connecting the two buildings is situated. In this part of the building, the dose rate in the technical gallery is less than $0.1 \mu\text{Sv/h}$ and on the gangway on the first floor is less than $1 \mu\text{Sv/h}$. The simulations predict that the radiation level on the gangway is particularly high: the maximum dose rate is $100 \mu\text{Sv/h}$. This value is unacceptable because the gangway is accessible to the members of the public (Fig. 6).

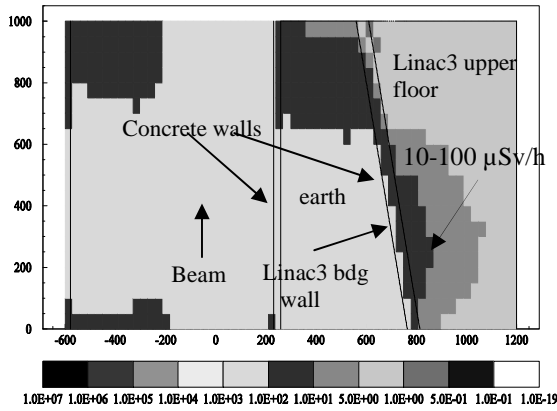


Fig 5 : Beam loss in a 5 x 5 x 5 cm³ copper target, 10 W, 140 MeV. Top cross sectional view of the Linac4 tunnel and of the Linac3 building. H*(10) in μSv/h at 530 cm, on the upper floor of the Linac3 building.

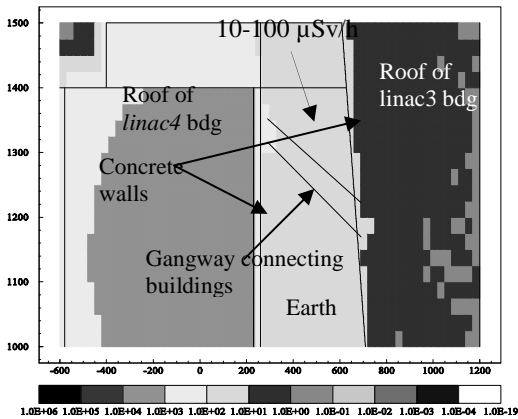


Fig 6: Beam loss in a 5 x 5 x 5 cm³ copper target, 10 W, 160 MeV. Top cross sectional view of the Linac4 tunnel and of Linac3 building. H*(10) in μSv/h at 760 cm above the hall floor where the gangway connecting the two buildings is located.

3. Waveguides duct studies for the green field solution

In the green field solution the Linac4 tunnel will be placed underground, so that the direct stray radiation is attenuated by the earthen shielding. The linac will effectively be shielded by about 4 m of earth plus about 1 m of concrete. The klystrons will be installed in an auxiliary tunnel located on the top of the linac tunnel and will be connected to the linac by waveguides running through ducts traversing the shielding. The first radiological simulation performed for the green field solution concerns the propagation

of neutrons through the waveguides ducts.

In the present design both the linac tunnel and the klystron tunnel are underground. The klystron gallery will be designed as a supervised radiation area according to CERN radiation Safety Manual [8] and the dose rate must be kept below 3 μSv/h. The shielding calculations were performed for the worst-case scenario (160 MeV, 10 W point losses every 10 m).

The stray radiation in the klystron tunnel is mainly given by the addition of two terms, the radiation propagating through the shield and the radiation streaming through the waveguides ducts. This study evaluates the minimum required earth thickness between the accelerator tunnel and the klystron tunnel and optimizes the number, cross-sectional area and length of the waveguides ducts.

For a point source calculation, the ambient dose equivalent rate H*(10) past the lateral shield approximates to

$$H = \frac{H_{\pi/2}}{r^2} e^{-\frac{d}{\lambda}}$$

where r is the distance from the radiation source to the exposure point of interest, H_{π/2} is the source term for 90 degrees emission, d is the shield thickness and λ is the attenuation length of the shielding material. The parameter r was assigned a value of 4 m. By scaling the values as in the Thomas and Stevenson book [9] to the losses in Linac4, it is found that at 160 MeV the source term for a 90 degrees emission is 1290 mSv/h and the attenuation length in concrete is 24.9 cm.

The concrete thickness required to reduce the dose equivalent rate down to 3 μSv/h is 254 cm. A safety factor of 3 in a shielding design is usually recommended. This can be obtained by increasing the concrete shielding by 1.1 λ, which leads to a 280 cm thickness of concrete. The minimum earth thickness required can approximately be assessed by simply scaling the thickness for concrete by the ratio of the densities of the two materials (taken as 1.8 g/cm³ for earth and 2.35 g/cm³ for concrete). Actually, the value used for the earth density should be regarded as conservative for local soil, a density of 2 g/cm³ being probably a more realistic figure. With this simplification, 280 cm of concrete are approximately equivalent to 370 cm of earth, from the point of view of radiation attenuation. As mentioned above, the shield is made of 100 cm of concrete plus 390 cm of earth and it is sufficient to reduce the dose-rate below 0.1 μSv/h.

Several Monte Carlo simulations were performed

to evaluate the transmission of neutrons through the waveguides ducts in order to assess the feasibility of grouping several waveguides in larger ducts. The cross-sectional area of the waveguides is $700 \times 250 \text{ mm}^2$. Two possible configurations for the ducts were studied :

- 1) several 200 cm long (in the beam direction) ducts, each one housing 2 waveguides,
- 2) one single 90 m long rectangular well housing all the 18 waveguides.

In both cases a three-legged configuration was considered. The width of the second leg increases from 40 cm to 60 cm in its upper part. The layout of the geometry used in the simulation is shown in Fig. 7

As shown in Fig. 8, for the 200 cm long duct in the most critical case the radiation streaming into the klystron tunnel is between 0.1 and $0.5 \mu\text{Sv/h}$. For the 90 m long rectangular well the dose streaming into the klystron tunnel can reach a maximum value between 1 and $3 \mu\text{Sv/h}$ (Fig. 9).

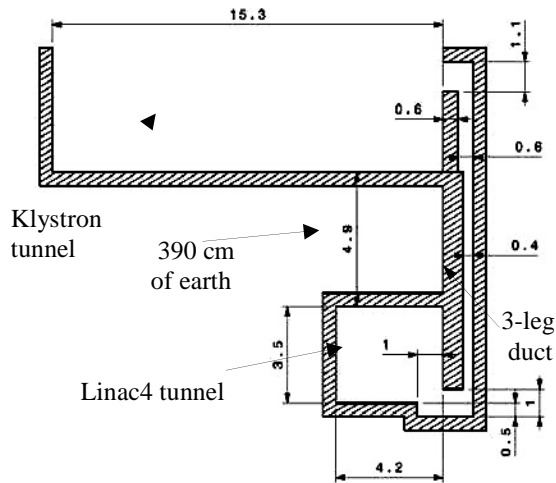


Fig 7: Layout of the geometry implemented in the simulation (linac tunnel, three-legged waveguides ducts and klystron tunnel).

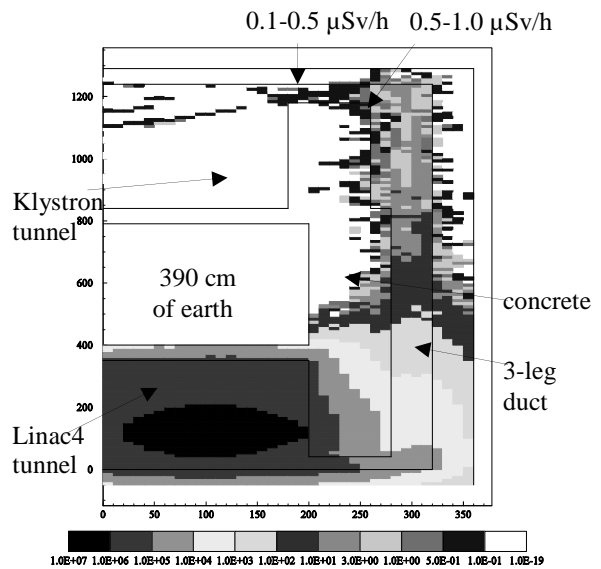


Fig 8: Beam loss in a $5 \times 5 \times 5 \text{ cm}^3$ copper target, 10 W, 160 MeV. Cross sectional view of the Linac4 tunnel, the 2 m long duct housing two waveguides and the klystron tunnel. $H^*(10)$ in $\mu\text{Sv/h}$.

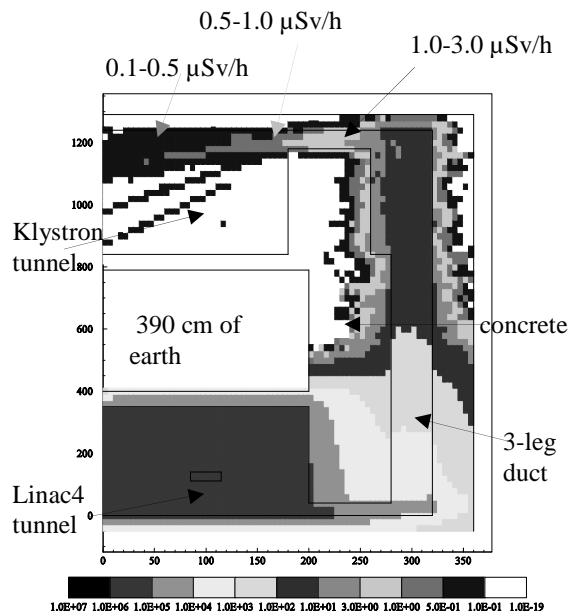


Fig 9: Beam loss in a $5 \times 5 \times 5 \text{ cm}^3$ copper target, 10 W, 160 MeV. Cross sectional view of the Linac4 tunnel, the 90 m long well housing all the waveguides and the klystron tunnel. $H^*(10)$ in $\mu\text{Sv/h}$.

4. Air activation

Three methods are commonly used for estimating induced radioactivity: 1) the multiplication of the density of inelastic interactions (“stars”) with pre-determined conversion factors, 2) the folding of particle track-length spectra with evaluated isotope production cross sections and 3) the explicit Monte Carlo calculation of isotope production from hadronic interaction models. The choice of the method depends on the case to be studied. Conversion factors from star densities are typically used for preliminary estimates and for bulk materials. Folding of track-lengths with energy-dependent cross sections is usually applied to low-density (e.g. gaseous) materials, as long as reliable experimental cross sections are available. The explicit calculation, which is relatively time-consuming, can assess the self-absorption in solids with complex geometry and the build-up and decay of radioactivity under arbitrary irradiation cycles. However, it fails in predicting induced radioactivity in gases due to the very low interaction probability.

The second approach was retained for the determination of air activation in the Linac4 tunnel. The track-length spectra were individually calculated by FLUKA for all air regions in the accelerator tunnel. The contribution from different regions were summed to obtain the total track-length spectra for neutrons, protons and charged pions. The yield Y_i of radionuclide i is then obtained by folding these spectra with energy-dependent partial cross-sections summed over all target nuclei and hadron components in the cascade

$$Y_i = \sum_{j,k} n_j \int \sigma_{ijk}(E) \Lambda_k(E) dE$$

Here n_j is the atomic concentration (per cm^3) of element j in the material and σ_{ijk} is the cumulative cross-section for the production of radionuclide i in the reaction of a particle of type k and energy E with a nucleus of element j . The quantity Λ_k is the sum of the track-lengths (in cm) of the hadrons of type k and energy E . A database with evaluated neutron, proton and charged pion interaction cross-sections which govern the conversion of the air constituents (^{14}N , ^{16}O and ^{40}Ar) into the radionuclide of interest by the various particles is available [10] and was used in a post-processing together with track-length spectra from the FLUKA simulations.

A section of the 91.5 m long accelerator tunnel was modelled with a cartesian geometry with beam direction along the z-axis. Most of the tunnel is air (density= 0.001205g/cm^3 , volume= $1.46 \times 10^9\text{cm}^3$) with the following composition (weight fraction): nitrogen

(75.558 %), oxygen (23.159 %) and argon (1.283 %). Assuming a beam loss of 1 W/m and a tunnel length of 90 m, the total beam loss in the tunnel is 90 W. This scenario was studied for three different beam energies: 50, 100 and 160 MeV. To evaluate the worker exposure during access after shutdown, the activities of airborne radionuclides have to be estimated based on the accelerator operating conditions. Assuming a continuous loss of a 90 W beam ($N_p=1.12 \cdot 10^{13}$ protons/s at 50 MeV; $N_p=5.62 \cdot 10^{12}$ protons/s at 100 MeV; $N_p=3.51 \cdot 10^{12}$ protons/s at 160 MeV), the saturation activity (A_s) for different radionuclides can be calculated from their yields: $A_s = Y N_p$. It was assumed that there is no ventilation during the operation and that the worker intervention lasts 1 hour. Several scenarios of irradiation and cooling times were considered. The activity for one single radionuclide after an irradiation time t_{irr} and a cooling time t_{cool} is:

$$A_0(t_{irr}, t_{cool}) = Y N_p (1 - e^{-\lambda t_{irr}}) e^{-\lambda t_{cool}}$$

If the activity is mixed homogeneously in the tunnel, the activity concentration is obtained by dividing the activity by the volume of air. To estimate the inhalation dose received by a worker it is necessary to multiply the calculated activities by the breathing rate B_r and the inhalation activity-to-dose conversion factors e_{inh} (expressed in Sv/Bq), which in the present study were taken from the Swiss ordonnance [11]:

$$D_0(t_{irr}, t_{cool}) = \frac{A_0(t_{irr}, t_{cool}) e_{inh} B_r}{V_{air}}$$

The standard breathing rate for a worker is $1.2\text{m}^3/\text{h}$. In order to estimate the total dose per intervention, the equation

$$D(t) = D_0(t_{irr}, t_{cool}) e^{-\lambda t}$$

should be integrated over the intervention time t_{int} . The inhalation dose received by a person intervening in the accelerator tunnel for t_{int} after a cooling time t_{cool} is:

$$D(t_{int}) = \frac{D_0(t_{irr}, t_{cool}) (1 - e^{-\lambda t_{int}})}{\lambda}$$

The values of inhalation doses obtained for the three scenarios (50, 100 and 160 MeV proton energy), with two irradiation times (1 day and 1 week) and three waiting times (0, 10 minutes and 1 hour) are given in Table 1. Only the nuclei that give relevant contribution to the dose are listed.

Table 1: Inhalation dose received by a worker intervening in the Linac4 tunnel.

Inhalation dose (μSv), $E_p = 50 \text{ MeV}$, intervention time = 1 hour, 90 W total proton beam loss in the tunnel						
t_{irr}	1 day	1 day	1 day	1 week	1 week	1 week
t_{cool}	0	10 min	1 hour	0	10 min	1 hour
^{11}C	5.63E-01	4.01E-01	7.33E-02	5.63E-01	4.01E-01	7.33E-02
^{38}Cl	2.34E-02	1.94E-02	7.66E-03	2.34E-02	1.94E-02	7.66E-03
^{39}Cl	2.35E-02	2.07E-02	1.11E-02	2.35E-02	2.07E-02	1.11E-02
^7Be	5.20E-02	5.20E-02	5.20E-02	3.50E-01	3.50E-01	3.50E-01
^{32}P	9.45E-02	9.45E-02	9.44E-02	5.75E-01	5.75E-01	5.74E-01
^{33}P	1.72E-02	1.72E-02	1.71E-02	1.11E-01	1.11E-01	1.11E-01
^{35}S	4.33E-03	4.33E-03	4.33E-03	2.96E-02	2.96E-02	2.96E-02
Total dose	7.83E-01	6.14E-01	2.64E-01	1.69E+00	1.52E+00	1.17E+00

Inhalation dose (μSv), $E_p = 100 \text{ MeV}$, intervention time = 1 hour, 90 W total proton beam loss in the tunnel						
t_{irr}	1 day	1 day	1 day	1 week	1 week	1 week
t_{cool}	0	10 min	1 h our	0	10 min	1 hour
^{11}C	2.37E-01	1.69E-01	3.08E-02	2.37E-01	1.69E-01	3.08E-02
^{38}Cl	2.43E-02	2.02E-02	7.97E-03	2.43E-02	2.02E-02	7.97E-03
^{39}Cl	4.52E-02	3.99E-02	2.14E-02	4.52E-02	3.99E-02	2.14E-02
^7Be	2.21E-02	2.21E-02	2.21E-02	1.49E-01	1.49E-01	1.49E-01
^{32}P	6.10E-02	6.09E-02	6.08E-02	3.71E-01	3.70E-01	3.70E-01
^{33}P	1.10E-02	1.10E-02	1.10E-02	7.14E-02	7.13E-02	7.13E-02
^{35}S	2.41E-03	2.41E-03	2.41E-03	1.65E-02	1.65E-02	1.65E-02
^{14}C	1.61E-03	1.61E-03	1.61E-03	1.13E-02	1.13E-02	1.13E-02
Total dose	4.08E-01	3.30E-01	1.60E-01	9.30E-01	8.52E-01	6.82E-01

Inhalation dose (μSv), $E_p = 160 \text{ MeV}$, intervention time = 1 hour, 90 W total proton beam loss in the tunnel						
t_{irr}	1 day	1 day	1 day	1 week	1 week	1 week
t_{cool}	0	10 min	1 hour	0	10 min	1 hour
^{11}C	1.37E-01	9.75E-02	1.78E-02	1.37E-01	9.75E-02	1.78E-02
^{38}Cl	4.43E-02	3.67E-02	1.45E-02	4.43E-02	3.67E-02	1.45E-02
^{39}Cl	8.62E-02	7.61E-02	4.08E-02	8.62E-02	7.61E-02	4.08E-02
^7Be	1.63E-02	1.63E-02	1.63E-02	1.10E-01	1.10E-01	1.10E-01
^{32}P	7.03E-02	7.02E-02	7.01E-02	4.27E-01	4.27E-01	4.26E-01
^{33}P	1.28E-02	1.28E-02	1.28E-02	8.25E-02	8.25E-02	8.24E-02
^{35}S	3.59E-03	3.59E-03	3.58E-03	2.45E-02	2.45E-02	2.45E-02
^{14}C	2.54E-03	2.54E-03	2.54E-03	1.78E-02	1.78E-02	1.78E-02
Total dose	3.83E-01	3.23E-01	1.84E-01	9.44E-01	8.83E-01	7.44E-01

5. Conclusions

In dealing with the installation of Linac4 in the present Linac2 building, it was not possible to use a simple analytical model for the estimation of the radiation levels due to the complexity of the geometry. Extensive Monte Carlo simulations proved to be the appropriate method to evaluate the transmission of stray radiation from Linac4 to Linac3. The FLUKA simulations predict that the installation of Linac4 in the Linac2 building would raise concern about the dose rate in two critical areas of Linac3: on the gangway connecting the two buildings and on the upper floor of the Linac3 building, where the dose equivalent rate can reach a maximum value of 100 $\mu\text{Sv/h}$. The existing amount of earth and the additional 40 cm thick layer of concrete between Linac3 and Linac4 are inadequate for reducing the dose rate to a value compatible with the CERN Safety Code [8] in all occupied areas.

The FLUKA simulations for the waveguide ducts for the green field solution lead to the conclusion that a 90 m long well housing all of the waveguides is a feasible solution. Slight modifications to the geometry could further reduce the ambient dose equivalent rate in the occupied areas.

Air activation studies were also performed for the green field solution, folding the particle track-lengths spectra obtained by Monte Carlo simulations with proper energy-dependent cross sections. This method was preferred to direct Monte Carlo calculations because of the low interaction probability of hadrons with air, which would lead to very large central processing unit (CPU) times. The inhalation dose received by workers during 1-hour maintenance operation in the tunnel was estimated for different irradiation cycles and waiting times, for 50, 100 and 160 MeV proton beam energy. The doses are similar at the three energies. They are slightly higher at 50 MeV because of the higher number of proton lost and because of the limited contribution of spallation products to gas activation in this energy range.

REFERENCES

- [1] L. Arnaudon et al, Linac4 Technical Design Report, M. Vretenar and F. Gerick, Editors, CERN-2006-AB-084 (2006).
- [2] B. Autin et al., Conceptual design of the SPL, a high power superconducting H^- linac at CERN, CERN Yellow Report 2000-012 (2000).
- [3] F. Gerick et al., Conceptual design of the SPL II, CERN Yellow Report 2006-006 (2006).
- [4] M. Magistris and M. Silari, Prompt radiation, shielding and induced radioactivity in a high-power 160 MeV proton linac. Nuclear Instruments and Methods A 562, 967-971, 2006.
- [5] A. Fassò, A. Ferrari, J. Ranft, and P.R. Sala, FLUKA: a multi-particle transport code, CERN-2005-10 (2005), INFN/TC_05/11, SLAC-R-773.
- [6] A. Fassò, A. Ferrari, S. Roesler, P.R. Sala, G. Battistoni, F. Cerutti, E. Gadioli, M.V. Garzelli, F. Ballarini, A. Ottolenghi, A. Empl and J. Ranft, The physics models of FLUKA: status and recent developments, Computing in High Energy and Nuclear Physics 2003 Conference (CHEP2003), La Jolla, CA, USA, March 24-28, 2003, (paper MOMT005), eConf C0303241 (2003), arXiv:hep-ph/0306267.
- [7] C. Theis, K.H. Buchegger, M. Brugger, D. Forkel-Wirth, S. Roesler and H. Vincke, Interactive three dimensional visualization and creation of geometries for Monte Carlo calculations, Nucl. Instrum. and Meth. A 562, 827-829 (2006).
- [8] CERN Safety Code F, Radiation Protection (November 2006).
- [9] R.H. Thomas and G.R. Stevenson, Radiological safety aspects of the operation of proton accelerators, Technical report n. 283, International Atomic Energy Agency, Vienna (1988).
- [10] M. Huhtinen, Determination of Cross Sections for Assessment of Air Activation at LHC, CERn/TIS-RP/TM/96-29 (1997).
- [11] Swiss Legislation on Radiological Protection (Ordonnance sur la Radioprotection, ORaP) of 22 June 1994 (state 4 April 2000).